A 2-Dimensional Finite-Element Method for Transient Magnetic Field Computation Taking Into Account Parasitic Capacitive Effects

W. N. Fu and S. L. Ho

***Abstract*—A formulation to model solid conductor groups in transient finite-element model (FEM) of inverter driven motor drives is presented to facilitate the users to model many solid conductors in one winding. A novel two-dimensional (2-D) FEM formulation which can include the displacement current in the direction of the model's depth is deduced. The effect of displacement current in the plane of the solution domain is represented by coupling the circuit of capacitances into the FEM equations. By introducing additional unknowns, the last set of the system equations has a symmetrical coefficient matrix. A method using electric charge as an excitation to compute the capacitance matrix is also presented to reduce the computation time. The developed algorithm has been applied to evaluate the effect of a LC filter in a converter motor drive and the parasitic capacitive effect is included.**

***Index Terms*—Electromagnetic field, finite-element method, motor, parasitic capacitance, power electronics, transient.**

I. Introduction

POWER electronic driven electric motors are providing a wealth of developmental opportunities to both designers and users of electric machines. However, these inverter drives also present new problems to researchers. Because of high speed switching and repetitive steep rising or falling in the voltage waveforms, there are inevitable high-frequency signals in these drives [1]–[3]. The parasitic capacitive effect and skin effect in the motor windings, which were insignificant in the past, are now becoming conspicuous to give rise to pronounced non-uniformities in the voltage distributions among the coils. The associated stresses due to the high derivative of voltage with respect to time are sources of premature winding insulation failures.

Because of the existing of very rich high-order harmonics in the motors, conventional analytical methods used to study electric machines operating under sinusoidal voltage excitations at power frequency cannot be used simply to consider the high-frequency effects of those drives excited by square wave voltages. As the switching frequency increases, the influence of eddy current in the magnetic cores and the skin effects on windings must be included if the electric machines and drives are to be modeled precisely. In [4] and [5], electric circuit models are used to simulate the traveling waves and voltage distribution in electric motors. The disadvantage of these modelings is that the eddy-current effect and nonlinear iron cores cannot be included. To consider the magnetic field distributions, finite difference methods are developed [6], [7]; and an eddy-current solver using FEM is proposed to simulate the magnetic field in frequency domain [8].

In order to study such transient issues, the most suitable method is to use time stepping FEM coupling with electric circuit to compute the magnetic fields and the circuit system simultaneously. However, such method is limited to model low-frequency problems mainly because the electric field is not coupled in most cases and the displacement current is ignored. To overcome this limitation, [9], [10] present a method which uses capacitances to include the effect of the displacement current. Reference [11] uses a similar method with the commercial software Maxwell 2D. To include the parasitic capacitive effect, all the coils are modeled as solid conductors. The capacitors are then connected among these conductors manually. However, this is a very time consuming process. Such methods cannot include the displacement current in the direction of the model's depth either.

In this paper a 2-D FEM is proposed to include the parasitic capacitive effect, eddy-current effect and arbitrarily connected external circuits. Many conductors can be grouped as one single winding and the users do not need to connect them manually. The proposed new FEM formulation includes the displacement current in the direction of the model's depth, and represents the displacement current effect in the 2-D plane of the solution domain by coupling capacitances among the conductors internally. For the computation of the capacitance matrix, a method using electric charge as an excitation is presented to reduce the computing time. The proposed algorithm has been used to simulate the transient problems of power electronic motor drives.

II. Modeling Method of Solid Conductors

To establish the basic equations of the electromagnetic field in motor drives, the following hypotheses are introduced: (i) The magnetic flux density $\vec{B}$ has components only in the $x-y$ plane. Therefore the magnetic vector potential $\vec{A}$ has a component only in the z direction, that is, $\vec{A} = A_z\vec{z}$; it is constant along the z axis. The coulomb gauge $\nabla \cdot \vec{A} = \partial A_z/\partial z = 0$ is satisfied. (ii) The conduction current flows along the z axis. (iii) The charge density is null.

Manuscript received October 20, 2009. This work was supported in part by The Hong Kong Polytechnic University under Grants 87RX, YH56 and B-Q18X.

W. N. Fu is with the Electrical Engineering Department, The Hong Kong Polytechnic University, Hong Kong (e-mail: eewnfu@polyu.edu.hk).

S. L. Ho is with the Electrical Engineering Department, The Hong Kong Polytechnic University, Hong Kong (e-mail: eeslho@polyu.edu.hk).

Color versions of one or more of the figures in this paper are available online at http://ieeexplore.ieee.org.

Digital Object Identifier 10.1109/TASC.2010.2042160

In the proposed method, the displacement currents along the z direction and in the $x-y$ plane will be all taken into account. The electric field can be decomposed into two orthogonal vectors:

$$\vec{E} = \vec{E}_z + \vec{E}_{xy} \tag{1}$$

The component E_z of electric field in the z direction:

$$E_z = -\frac{\partial A}{\partial t} - \frac{\partial V}{\partial z} \tag{2}$$

where V is the electric scalar potential of the conductor in the domain of magnetic field. Equation (2) implies that the changing magnetic field and the electric scalar potential are producing electric field in the z direction. If u_c is the voltage drop between the two terminals of the conductor which has a length l in the z direction, one has:

$$\frac{\partial V}{\partial z} = -\frac{d_c}{l} u_c \tag{3}$$

where d_c is the polarity ($+1$ or -1) representing either the forward or return paths. Substituting (3) into (2) gives:

$$E_z = -\frac{\partial A}{\partial t} + \frac{d_c}{l} u_c \tag{4}$$

According to the hypotheses, the components A_x and A_y are neglected, hence:

$$\vec{E}_{xy} = -(\nabla V)_{xy} \tag{5}$$

It means that the magnetic field has no direct effect upon the electric field on the $x-y$ plane.

According to $\nabla \cdot \vec{D} = \rho$ and $\vec{D} = \varepsilon \vec{E}$, therefore:

$$\nabla \cdot \vec{D}_{xy} = \nabla \cdot \varepsilon \vec{E}_{xy} = -\nabla \cdot (\varepsilon \nabla V)_{xy} = \rho \tag{6}$$

On the outside of the conductors, the charge density $\rho = 0$. In the conductors, the electric relaxation time $\tau = \varepsilon/\sigma$ ($= 8.854 \times 10^{-12}$ F/m$/5.8 \times 10^{7}$ Siemens/meter in copper) is very small, hence it is assumed that $\rho = 0$. Each conductor is thus an equal-potential region in the $x-y$ plane [12].

According to (6), the electric field equation on the $x-y$ plane is:

$$-\nabla_{xy} \cdot (\varepsilon \nabla_{xy} V) = 0 \tag{7}$$

The alternating electric vector displacement E_z will generate displacement current density J_{dz} in the z direction; J_{dz} generates A_z, which means the changing electric field generates a magnetic field in the $x-y$ plane; E_{xy} will generate the displacement current density J_{dxy} in $x-y$ plane, then J_{dxy} also generates A_{xy}. In the 2-D FEM of radial-field electric motors, the influence of A_{xy} is negligible.

According to the Maxwell-Ampere's law:

$$\nabla \times (\nu \nabla \times \vec{A}) = \sigma \vec{E} + \varepsilon \frac{\partial \vec{E}}{\partial t} \tag{8}$$

and

$$\nabla \times (\nu \nabla \times \vec{A}) = -\nabla_{xy} \cdot (\nu \nabla_{xy} A_z) \tag{9}$$

Hence:

$$-\nabla_{xy} \cdot (\nu \nabla_{xy} A) + \sigma \frac{\partial A}{\partial t} + \sigma \frac{\partial V}{\partial z} - \varepsilon \frac{\partial}{\partial t} \left(-\frac{\partial A}{\partial t} - \frac{\partial V}{\partial z} \right) = 0 \tag{10}$$

where A_z is simplified as A; ν is the reluctivity of the material and σ is the conductivity.

Substituting (3) into (10), the local magnetic field equation in the conductor can be written as:

$$-\nabla_{xy} \cdot (\nu \nabla_{xy} A) + \sigma \frac{\partial A}{\partial t} - \frac{d_c \sigma}{l} u_c + \varepsilon \frac{\partial^2 A}{\partial t^2} - \frac{d_c \varepsilon}{l} \frac{\partial u_c}{\partial t} = 0 \tag{11}$$

The total current density in the conductor along the direction of the z axis is:

$$J_z = -d_c \sigma \frac{\partial A}{\partial t} - \sigma \frac{u_c}{l} + \varepsilon \frac{\partial}{\partial t} \left(-d_c \frac{\partial A}{\partial t} + \frac{u_c}{l} \right) \tag{12}$$

The total current in the conductor along the z axis is:

$$\begin{aligned} i_c &= \iint_{\Omega_c} \left[\sigma \left(-d_c \frac{\partial A}{\partial t} + \frac{u_c}{l} \right) + \varepsilon \left(-d_c \frac{\partial^2 A}{\partial t^2} + \frac{\partial}{\partial t} \frac{u_c}{l} \right) \right] \mathrm{d}\Omega \\ &= -d_c \sigma \iint_{\Omega_c} \frac{\partial A}{\partial t} \mathrm{d}\Omega + \sigma \frac{\iint_{\Omega_c} \mathrm{d}\Omega}{l} u_c + \iint_{\Omega_c} \varepsilon \left(-d_c \frac{\partial^2 A}{\partial t^2} + \frac{\partial}{\partial t} \frac{u_c}{l} \right) \mathrm{d}\Omega \\ &= e_c + \frac{1}{R_c} u_c + \iint_{\Omega_c} \varepsilon \left(-d_c \frac{\partial^2 A}{\partial t^2} + \frac{\partial}{\partial t} \frac{u_c}{l} \right) \mathrm{d}\Omega \end{aligned} \tag{13}$$

where the resistance of the conductor is:

$$R_c = \frac{l}{\sigma \int \int_{\Omega_c} \mathrm{d}\Omega} = \frac{l}{\sigma S_c} \tag{14}$$

where $S_c = \int \int_{\Omega_c} \mathrm{d}\Omega$ is the cross-sectional area of the conductor.

The back e.m.f. of the conductor is:

$$e_c = -d_c \sigma \iint_{\Omega_c} \frac{\partial A}{\partial t} \mathrm{d}\Omega \tag{15}$$

For simplicity, the electrostatic field described by (7) is solved before the capacitance matrix is extracted. The current flowing out from the n^{th} conductor in the $x-y$ plane can be computed by:

$$i_{xyn} = \sum_{k=1}^{\text{All conductors}} C_{nk} \frac{\mathrm{d}u_{nk}}{\mathrm{d}t} \tag{16}$$

The electrostatic field with multi right hand sides (see Section III) only needs to be computed once if there is no motion. Under such condition, only the electric circuit with all these capacitances, instead of the electric field, needs to be coupled with the magnetic field directly.

To overcome the problem that (11) includes the second derivative of A with respect to time t, and to keep the coefficient matrix of the last system equations symmetrical, the unknown E_z is kept in the system equation. Multiplying ε to the two sides of (4) gives:

$$-\varepsilon \frac{\partial A}{\partial t} - \varepsilon E_z + \frac{d_c \varepsilon}{l} u_c = 0 \tag{17}$$

According to (4) and (11),

$$-\nabla_{xy} \cdot (\nu \nabla_{xy} A) + \sigma \frac{\partial A}{\partial t} - \varepsilon \frac{\partial E_z}{\partial t} - \frac{d_c \sigma}{l} u_c = 0 \tag{18}$$

According to (13),

$$-\frac{d_c \sigma}{l} \iint_{\Omega_c} \frac{\partial A}{\partial t} \mathrm{d}\Omega + \frac{1}{l R_c} u_c + \frac{d_c \varepsilon}{l} \iint_{\Omega_c} \frac{\partial E_z}{\partial t} \mathrm{d}\Omega = \frac{1}{l} i_c \tag{19}$$

The system equations in regions of solid conductors are (18), (17) and (19).

Periodic boundary conditions can be used to reduce the solution domain. Similar to the stranded windings, the solid conductors should also be grouped together if their electric and magnetic field quantities satisfy either periodic condition or anti-periodic condition [13]. The basic relationships between one conductor and the conductor group are:

$$S_c = \frac{pS_w}{N_w} \tag{20}$$

$$i_c = \frac{i_w}{a} \tag{21}$$

$$d_c u_c = \frac{d_w a}{N_w} u_w \tag{22}$$

$$R_c = \frac{a^2}{N_w} R_w \tag{23}$$

where p is the symmetry multiplier which is defined as the ratio of the original full cross-sectional area to the solution area, $S_w = \int\int_{\Omega_w} \mathrm{d}\Omega$ the total cross-sectional area of the region occupied by this conductor group in the solution domain, u_w the voltage difference between the two terminals of the solid conductor group, i_w the total current, N_w the total conductor number, a the number of parallel branches and R_w is the d.c. resistance of the conductor group.

Substituting (22) into (18), the field equation in the solid conductor group is:

$$-\nabla_{xy} \cdot (\nu \nabla_{xy} A) + \sigma \frac{\partial A}{\partial t} - \varepsilon \frac{\partial E_z}{\partial t} - \frac{d_w a \sigma}{N_w l} u_w = 0 \tag{24}$$

Substituting (22) into (17) gives:

$$-\varepsilon \frac{\partial A}{\partial t} - \varepsilon E_z + \frac{d_w a \varepsilon}{N_w l} u_w = 0 \tag{25}$$

Substituting (20), (21), (22) and (23) into (19), the circuit branch equation of the solid conductor group is:

$$-\frac{d_w a \sigma}{N_w l} \iint\limits_{\Omega_w} \frac{\partial A}{\partial t} \mathrm{d}\Omega + \frac{1}{lpR_w} u_w + \frac{d_w a \varepsilon}{N_w l} \iint\limits_{\Omega_w} \frac{\partial E_z}{\partial t} \mathrm{d}\Omega = \frac{1}{lp} i_w \tag{26}$$

Therefore, the system equations in the region of the solid conductors are (24), (25) and (26).

Basic equations in the airgap, iron cores, permanent magnet (PM) materials and stranded windings have been presented in [13]. The basic equations in all regions can be summarized as:

$$-\nabla_{xy} \cdot (\nu \nabla_{xy} A) + \sigma \frac{\partial A}{\partial t} - \varepsilon \frac{\partial E_z}{\partial t} + \frac{d_w a \sigma}{N_w l} e - \frac{d_w a \sigma}{N_w l} u_w = J_s - \nu \mu_0 \left(\frac{\partial M_x}{\partial y} - \frac{\partial M_y}{\partial x} \right) \tag{27}$$

$$-\varepsilon \frac{\partial A}{\partial t} - \varepsilon E_z + \frac{d_w a \varepsilon}{N_w l} u_w = 0 \tag{28}$$

$$\frac{d_w a \sigma}{N_w l} \iint\limits_{\Omega_w} \frac{\partial A}{\partial t} \mathrm{d}\Omega - \frac{1}{lpR_w} e = 0 \tag{29}$$

$$-\frac{d_w a \sigma}{N_w l} \iint\limits_{\Omega_w} \frac{\partial A}{\partial t} \mathrm{d}\Omega + \frac{d_w a \varepsilon}{N_w l} \iint\limits_{\Omega_w} \frac{\partial E_z}{\partial t} \mathrm{d}\Omega + \frac{1}{lpR_w} u_w = \frac{1}{lp} i_w \tag{30}$$

where i_w is the current in the stranded windings or the solid conductor groups and u_w the voltage difference between the two terminals of the stranded windings or the solid conductor groups. M_x and M_y are, respectively, the x and y components of the magnetization vector (amperes/meter) in the PM. The fourth term on the left side of (27), and also (29) exist only in the stranded winding region. The second and the third terms on the left side of (27), (28), and the second term in (30) only exist in the solid conductor region.

The capacitances among the conductors are computed by using electrostatic field solver and are coupled automatically with FEM as an internal coupling. The power electronic circuit is coupled with FEM as an external coupling [13]. The last coefficient matrix of FEM is symmetrical.

III. Capacitance Matrix Computation

The electric filed equation on the $x - y$ plane is (7). If the system has N conductors, usually the capacitances are computed by solving the field equations N times when setting the voltage potentials as: $(V_1, V_2, \ldots, V_N) = (1, 0, \ldots, 0), (0, 1, \ldots, 0), \ldots$, and $(0, 0, \ldots, 1)$, respectively (here $V_1, V_2, \ldots, V_N$ are the voltage potentials on conductor 1, 2, ..., and N, respectively). Because such setting of the voltage potentials is considered as constraints in (7), one needs to establish and solve the FEM equations N times.

Here the charge excitation is presented to calculate the capacitances. Because of the relationship of $Q = CV$, the net charge on each object [see (31) shown at the bottom of the page]

By defining a G matrix:

$$\begin{bmatrix} G_{11} & G_{12} & \cdots & G_{1N} \\ G_{21} & G_{22} & \cdots & G_{2N} \\ \cdots & \cdots & \cdots & \cdots \\ G_{N1} & G_{N2} & \cdots & G_{NN} \end{bmatrix} = \begin{bmatrix} C_{11} & -C_{12} & \cdots & -C_{1N} \\ -C_{21} & C_{22} & \cdots & -C_{2N} \\ \cdots & \cdots & \cdots & \cdots \\ -C_{N1} & -C_{N2} & \cdots & C_{NN} \end{bmatrix}^{-1} \tag{32}$$

$$\begin{Bmatrix} Q_1 \\ Q_2 \\ \vdots \\ Q_N \end{Bmatrix} = \begin{bmatrix} C_{10} + C_{12} + \cdots + C_{1N} & -C_{12} & \cdots & -C_{1N} \\ -C_{21} & C_{20} + C_{21} + \cdots + C_{2N} & \cdots & -C_{2N} \\ \cdots & \cdots & \cdots & \cdots \\ -C_{N1} & -C_{N2} & \cdots & C_{N0} + C_{N1} + \cdots + C_{N(N-1)} \end{bmatrix} \begin{Bmatrix} V_1 \\ V_2 \\ \vdots \\ V_N \end{Bmatrix}$$

$$= \begin{bmatrix} C_{11} & -C_{12} & \cdots & -C_{1N} \\ -C_{21} & C_{22} & \cdots & -C_{2N} \\ \cdots & \cdots & \cdots & \cdots \\ -C_{N1} & -C_{N2} & \cdots & C_{NN} \end{bmatrix} \begin{Bmatrix} V_1 \\ V_2 \\ \vdots \\ V_N \end{Bmatrix} \tag{31}$$

we have:

$$\begin{Bmatrix} V_1 \\ V_2 \\ \vdots \\ V_N \end{Bmatrix} = \begin{bmatrix} C_{11} & -C_{12} & \cdots & -C_{1N} \\ -C_{21} & C_{22} & \cdots & -C_{2N} \\ \cdots & \cdots & \cdots & \cdots \\ -C_{N1} & -C_{N2} & \cdots & C_{NN} \end{bmatrix}^{-1} \begin{Bmatrix} Q_1 \\ Q_2 \\ \vdots \\ Q_N \end{Bmatrix} = \begin{bmatrix} G_{11} & G_{12} & \cdots & G_{1N} \\ G_{21} & G_{22} & \cdots & G_{2N} \\ \cdots & \cdots & \cdots & \cdots \\ G_{N1} & G_{N2} & \cdots & G_{NN} \end{bmatrix} \begin{Bmatrix} Q_1 \\ Q_2 \\ \vdots \\ Q_N \end{Bmatrix} \quad (33)$$

If the charge excitations are set as:

$$\{Q_1 \quad Q_1 \quad \cdots \quad Q_N\}^T = \{1 \quad 0 \quad \cdots \quad 0\}^T \quad (34)$$

Then:

$$\begin{bmatrix} V_1 \\ V_2 \\ \vdots \\ V_N \end{bmatrix} = \begin{bmatrix} G_{11} & G_{12} & \cdots & G_{1N} \\ G_{21} & G_{22} & \cdots & G_{2N} \\ \cdots & \cdots & \cdots & \cdots \\ G_{N1} & G_{N2} & \cdots & G_{NN} \end{bmatrix} \begin{bmatrix} 1 \\ 0 \\ \vdots \\ 0 \end{bmatrix} \quad (35)$$

After the field is solved, $V_1, V_2, \ldots$, and V_N are known. One column of G matrix is obtained:

$$\{G_{11} \quad G_{21} \quad \cdots \quad G_{N1}\}^T = \{V_1 \quad V_2 \quad \cdots \quad V_N\}^T \quad (36)$$

Similarly, if the charge excitations are set as:

$$\{Q_1 \quad Q_1 \quad \cdots \quad Q_N\}^T = \{0 \quad 1 \quad \cdots \quad 0\}^T \quad (37)$$

we have:

$$\{G_{12} \quad G_{22} \quad \cdots \quad G_{N2}\}^T = \{V_1 \quad V_2 \quad \cdots \quad V_N\}^T \quad (38)$$

If the charge excitations are set as:

$$\{Q_1 \quad Q_1 \quad \cdots \quad Q_N\}^T = \{0 \quad 0 \quad \cdots \quad 1\}^T \quad (39)$$

we have:

$$\{G_{13} \quad G_{23} \quad \cdots \quad G_{NN}\}^T = \{V_1 \quad V_2 \quad \cdots \quad V_N\}^T \quad (40)$$

After the G matrix is obtained, the C matrix can be obtained using (32). With this algorithm, the coefficient matrix of the FEM equations can be kept unchanged. Only a multi right hand side (RHS) problem needs to be solved. By using the multi-RHS algebraic solvers, the computing time required to extract the capacitance matrix can be greatly reduced.

IV. Application Example

The developed FEM is applied to evaluate the effects of a LC filter of an inverter driven 250 kW, 380 V, 2-pole, 50 Hz induction motor (Fig. 1). The carrier frequency of pulse-width-modulation (PWM) is 4 kHz. Step voltages representing the PWM wavefronts with a rise-time of 50 ns and a magnitude of 400 V are applied to the windings. The responses of the nodal voltages on the conductors are shown in Fig. 2. It reveals that the voltage drops on the conductors are non-uniform as the rise-time is very short because of capacitance effect. The responses of the nodal voltages with a Γ-shaped LC filter (40 mH, 60 μF) connected between the output of the inverter and the stator windings are shown in Fig. 3. It can be seen that the LC filter makes the voltage drops on the stator windings more uniform.

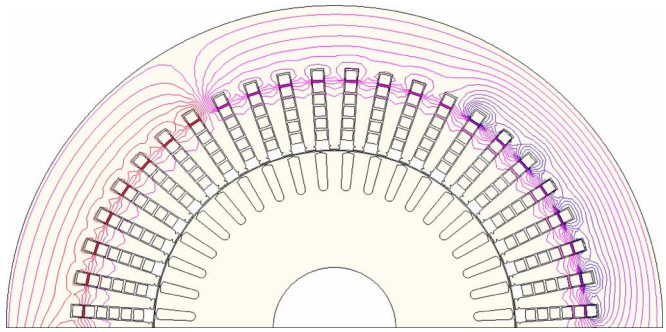

Fig. 1. The cross-section of an induction motor and its flux plot at $t = 2 \times 10^{-8}$ s.

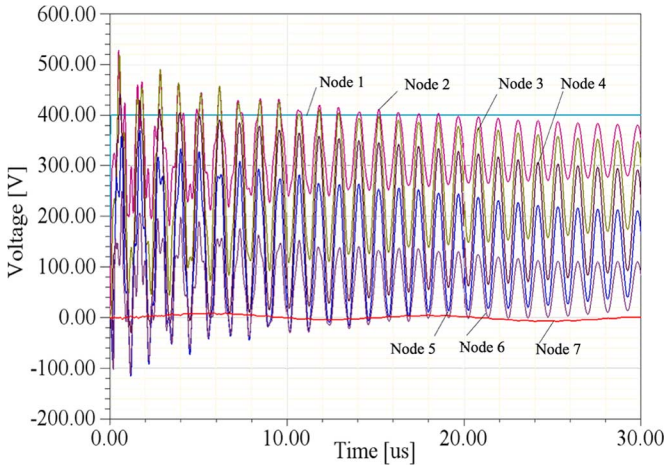

Fig. 2. The nodal voltages when no filter is connected.

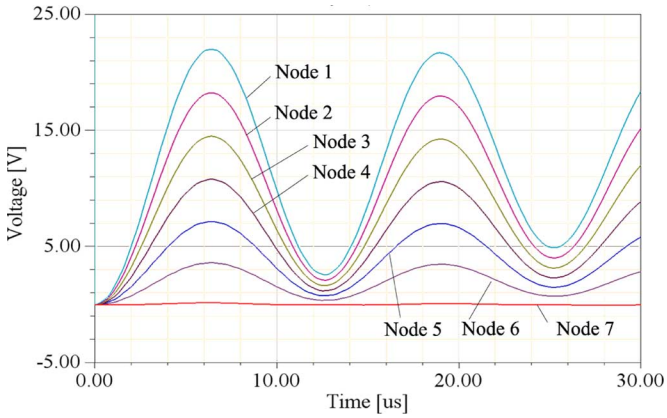

Fig. 3. The nodal voltages when a filter is connected.

V. Conclusion

The proposed 2-D FEM for the electromagnetic field computation of power electronic drives can include the displacement current in the model's depth; the effect of displacement current on the plane of the solution domain is included by coupling the capacitance circuit with FEM equations. The capacitance matrix

can be extracted by solving the electric field equations driven by charges, hence only a set of equations with multi right hand sides needs to be solved for the capacitance matrix computation. The developed methods are used to simulate the operation of inverter-driven motors.

REFERENCES

[1] M. Moreau, N. Idir, and P. Le Moigne, "Modeling of conducted EMI in adjustable speed drives," *IEEE Trans. Electromagnetic Compatibility*, vol. 51, no. 3, pt. 2, pp. 665–672, Aug. 2009.

[2] A. Videt, P. Le Moigne, N. Idir, P. Baudesson, J.-J. Franchaud, and J. Ecrabey, "Motor overvoltage limitation by means of a new EMI-reducing PWM strategy for three-level inverters," *IEEE Trans. Industry Applications*, vol. 45, no. 5, pp. 1678–1687, Sept.–Oct. 2009.

[3] U. T. Shami and H. Akagi, "Experimental discussions on a shaft end-to-end voltage appearing in an inverter-driven motor," *IEEE Trans. Power Electronics*, vol. 24, no. 6, pp. 1532–1540, June 2009.

[4] L. Gubbala, A. von Jouanne, P. N. Enjeti, C. Singh, and H. A. Toliyat, "Voltage distribution in the windings of an ac motor subjected to high dv/dt PWM voltages," in *IEEE PESC Conf. Proc.*, 1995, pp. 579–585.

[5] Hussain and G. Joos, "Modeling and simulation of traveling waves in induction motor drives," in *IEEE APEC Conf. Rec.*, 1997, pp. 128–134.

[6] D. B. Hyypio, "Simulation of cable and winding response to steep-fronted voltage waves," in *IEEE IAS Conf. Rec.*, 1995, pp. 800–806.

[7] Y. Tang, "Analysis of steep-fronted voltage distribution and turn insulation failure in inverter fed ac motor," in *IEEE IAS Conf. Rec.*, 1997, pp. 509–516.

[8] G. Suresh, H. A. Toliyat, D. A. Rendusara, and P. N. Enjeti, "Predicting the transient effects of PWM voltage waveform on the stator windings of random wound induction motors," *IEEE Trans. Power Electronics*, vol. 14, no. 1, pp. 23–30, Jan. 1999.

[9] J. S. Lai, X. D. Huang, E. Pepa, S. T. Chen, and T. W. Nehl, "Inverter EMI modeling and simulation methodologies," *IEEE Trans. Industrial Electronics*, vol. 53, no. 3, pp. 736–744, June 2006.

[10] J. F. Charpentier, Y. Lefevre, and M. Lajoie-Mazenc, "A 2D finite element formulation for the study of the high frequency behaviour of wound components," *IEEE Trans. Magn.*, vol. 32, no. 3, pp. 1098–1101, May 1996.

[11] H. A. Toliyat, G. Suresh, and A. Abur, "Simulation of voltage stress on the inverter fed induction motor windings supplied through feeder cable," in *IEEE IAS Conf. Rec.*, 1997, pp. 143–150.

[12] R. Miller, D. M. Ryder, and K. J. Overshott, "The effect of high-voltage lightning impulses on the core properties of transformers," *IEEE Trans. Magn.*, vol. 25, no. 5, pp. 3988–3990, Sept. 1989.

[13] W. N. Fu, P. Zhou, D. Lin, S. Stanton, and Z. J. Cendes, "Modeling of solid conductors in two-dimensional transient finite-element analysis and its application to electric machines," *IEEE Trans. Magn.*, vol. 40, no. 2, pp. 426–434, March 2004.